Unraveling the Temperature-Dependent Relaxation Dynamics of Ionic Liquid-Plasticized Complexmers

van Lange, Sophie G.M.; Biella, Riccardo; te Brake, Diane W.; Dol, Sinty; Besten, Maarten; Sprakel, Joris; Garcia, Santiago J.; van der Gucht, Jasper

DOI
10.1021/acs.macromol.5c01318

Publication date
2025

Document Version
Final published version

Published in
Macromolecules

Citation (APA)
van Lange, S. G. M., Biella, R., te Brake, D. W., Dol, S., Besten, M., Sprakel, J., Garcia, S. J., & van der Gucht, J. (2025). Unraveling the Temperature-Dependent Relaxation Dynamics of Ionic Liquid-Plasticized Complexmers. *Macromolecules*, *58*(14), 7522-7533. https://doi.org/10.1021/acs.macromol.5c01318

Macromolecules

pubs.acs.org/Macromolecules
Article

Unraveling the Temperature-Dependent Relaxation Dynamics of Ionic Liquid-Plasticized Complexmers

Sophie G. M. van Lange,* Riccardo Biella, Diane W. te Brake, Sinty Dol, Maarten Besten, Joris Sprakel, Santiago J. Garcia, and Jasper van der Gucht*

Cite This: https://doi.org/10.1021/acs.macromol.5c01318
Read Online

ABSTRACT: Polyelectrolytes with ionic domains screened by bulky hydrophobic segments form processable, hydrophobic complexes called "complexmers". Ionic liquids, which are chemically similar, further plasticize complexmers, yet the mechanisms behind their plasticization effects and distribution within the complexes remain unclear. This study examines the relaxation dynamics of plasticized complexmers across multiple length scales using rheology, fluorescence recovery after photobleaching (FRAP), and broadband dielectric spectroscopy (BDS). The incorporation of ionic liquids into complexmers reduces their glass transition temperature (T_g), accelerates diffusive processes, increases segmental motion, and leads to a small decrease in activation energy associated with these relaxation processes. However, the activation energies vary substantially between techniques, probing different physical processes: approximately 200 kJ/mol in rheology, 50 kJ/mol in FRAP, and 90 kJ/mol in BDS. These variations suggest that collective dynamics strongly influence the complexmer rheology, making the mobilization (and activation) of polymer chains distinct from the local movement of ionic segments.

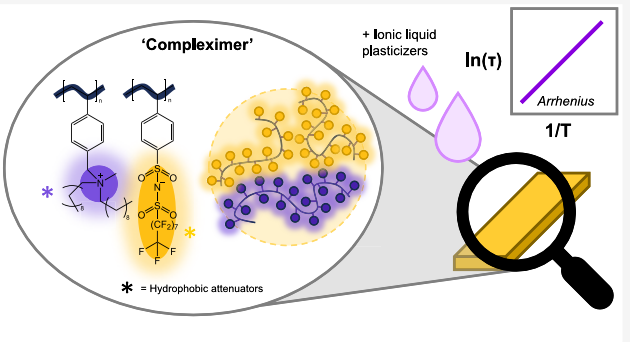

INTRODUCTION

Nature effectively utilizes ionic interactions to structure and strengthen materials. Organisms like sandcastle worms[1] and velvet worms,[2] for example, have evolved to exploit the attraction between opposite charges to create underwater adhesives and biological slimes. Based on the same interactions, cellular compartmentalization in membraneless organelles in cells arises from the complexation of charged RNA and proteins.[3] The prevalence and diversity of charged macromolecules in nature can lead to the formation of complex yet highly functional materials. Capturing this functionality in synthetic systems has remained largely limited to the formation of moderately hydrated polyelectrolyte complexes (PECs),[4] and liquid complex coacervates[5] from mixing solutions of (synthetic) polyelectrolytes. In nature, PECs form and operate in highly hydrated environments, where water and dissolved salts act as plasticizers by screening the electrostatic interactions.[6,7] In the lab, it has been challenging to synthetically produce PECs that break free from their plasticized environment and, rather than being sticky or slimy, harness ionic interactions as (reversible) cross-linkers, mimicking the behavior of covalent bonds in thermosetting plastics. In addition to their sensitivity to moisture, dried PECs are extremely brittle and challenging to process due to the absence of a glass transition.[8]

We have previously shown, however, that introducing hydrophobic segments into the polyelectrolyte structure enables the creation of PECs that resist hydration, and referred to these as "complexmers".[9] By incorporating bulky, hydrophobic domains near charged groups, complexmers achieve an internal plasticizing effect, reducing rigidity, lowering the glass transition temperature (T_g) and thus enabling processability at elevated temperatures below the degradation temperature and without water. This innovation results in a hydrophobic, physically cross-linked material that combines thermoplastic-like recyclability with the network stability of thermosets, based on ionic interactions.

These complexmers were found to exhibit a very broad thermal transition, extending to temperatures that are close to the degradation temperature of the polymers. The glass transition temperature could be lowered further by adding external plasticizers, which allowed us to capture the full transition. The bulky ions in complexmers are molecularly very similar to ionic liquids, a class of organic salts that are fluid

Received: May 16, 2025
Revised: July 2, 2025
Accepted: July 2, 2025

https://doi.org/10.1021/acs.macromol.5c01318
Macromolecules XXXX, XXX, XXX−XXX

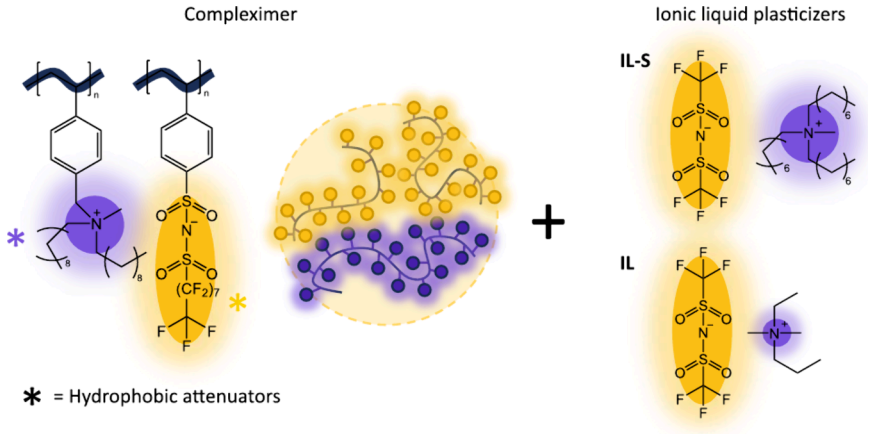

Figure 1. Schematic of polystyrene based complexiners plasticized with ionic liquids. IL-S is a bulky ionic liquid with a polycation screened by long hydrocarbon spacers. IL is a small molecule ionic liquid.

at temperatures typically below 100 °C.[10] We therefore found ionic liquids to be very effective plasticizers of complexiners, lowering their T_g and rendering them flexible under mild heating.[9] Plasticization in polymeric materials typically occurs through the addition of small molecules that enhance flexibility by lubricating the polymer chains by reducing friction, disrupting intermolecular interactions, and/or increasing free volume.[11] In PECs, the water content[6,12] (controlled through modulating the relative humidity) and the salt concentration[13,14] affect the energy barriers for the relaxation, which has been described previously by time-water and time−salt superpositions. The precise mechanism by which ionic liquids facilitate plasticization in water-free complexiners and how they are distributed within the complexiner matrix has remained unexplored.

In this work, we employ several experimental techniques to unveil the relaxation behavior of complexiners plasticized with ionic liquids (Schematic, Figure 1). Time−temperature superposition (TTS) applied to the rheology data obtained from oscillation experiments allows us to construct master curves of viscoelastic behavior by shifting data obtained at different temperatures, offering insights into the material's bulk relaxation behavior. Fluorescence lifetime imaging microscopy (FLIM) and fluorescence recovery after photobleaching (FRAP) are used to study the microstructure and dynamics of the material, providing insights into the distribution and movement of small molecules within the complexiner. Broadband dielectric spectroscopy (BDS), here used in combination with TTS, probes the material's response to an oscillating electric field, allowing us to study the frequency-dependent molecular dynamics and dielectric properties, which are closely related to the mobility of ionic and polymeric species. These techniques reveal that ionic liquids lower the material's T_g and accelerate its dynamics, resembling a unique Arrhenius-type relaxation that has only been observed in organic vitrimer materials.[15] Plasticization has a minimal impact on the fundamental relaxation processes in complexiners, as the activation energies change only moderately, regardless of plasticizer type or content. However, significant discrepancies in activation energies are observed between the different methods, which probe different relaxation phenomena. This suggests that in complexiners, relaxations on large scale, where cooperative effects play a role, are different from the mobility of small molecules and local movements.

EXPERIMENTAL SECTION

Sample Preparation. The synthesis and processing of screened (S) complexiners, including the addition of plasticizers dioctyl phthalate (DOP), as well as two ionic liquids: screened methyl-trioctylammonium bis(trifluoromethylsulfonyl)imide (IL-S) and nonscreened ethyldimethylpropylammonium bis(trifluoromethyl-sulfonyl)imide (IL) was described in our previous work.[9]

Dynamic Mechanical Analysis (DMA). We here prepared samples with dimensions 2 × 0.5 × 0.1 cm for use in extensional DMA. For DMA in shear, we prepared samples with a diameter of 1 cm and a thickness of approximately 0.1 cm. Samples with 0% ionic liquid and 5% DOP were performed in extension. Samples with 10% and 20% IL-S and 35% IL were performed in shear. Extensional moduli were converted to shear moduli assuming a Poisson ratio of 0.5, so that E = 3G, which shows excellent agreement (Figure S1). We apply the time temperature superposition (TTS) principle to frequency sweeps recorded at a range of temperatures, using an Anton Paar 702 Space Multidrive. The extensional DMA fixture was used for extensional oscillatory measurements on the rectangular complexiner samples. The round samples were measured with a 10 mm in diameter crosshatched plate−plate geometry.

Time Temperature Superposition (TTS). After fixing the sample in the DMA, a temperature equilibration was performed at 170 °C for 10 min prior to the measurement to ensure full equilibration, and adhesion to the parallel plate when used. Subsequently, frequency sweeps were performed from 170 to 40 °C in steps of 10 °C. Between each measurement, the new temperature was held for 5 min to ensure proper equilibration. The frequency sweep experiments ran between 10^2 and 10^{-1} rad s^{-1} (or 10^2 and 10^0 rad s^{-1} for the samples with 35% IL-S, DOP plasticized samples) while oscillating with a strain of 0.01%. In extension, a preload force of 1500 Pa was applied, and in shear, a Normal force of 2 N was applied. Mastercurves were then constructed through shifting the moduli and tanδ values horizontally by multiplying the frequency axis with a temperature dependent shift factor a_T relative to the reference temperature of 120 °C. The activation energies were extracted by fitting to the Arrhenius equation.

Fluorescence Lifetime Imaging (FLIM). *Sample Preparation.* Fluorescently labeled samples, including ionic liquids, were prepared by swelling powdered complexiner powder in dimethylformamide (DMF) containing a stock solution of Azido Bodipy[16] and a desired amount of ionic liquid. The final Bodipy content in the dried complexiner film was calculated to be 0.001%. Upon overnight swelling, the DMF was removed with a rotary evaporator, after which the powder was further dried in a vacuum oven. When fully dried, the powder was placed between two Teflon sheets and hot-pressed at 110 °C to obtain thin complexiner films. These films were transferred to object glasses.

FLIM Measurements. Fluorescence lifetime imaging microscopy (FLIM) was performed on a Leica TCS SP8 inverted confocal

https://doi.org/10.1021/acs.macromol.5c01318
Macromolecules XXXX, XXX, XXX−XXX

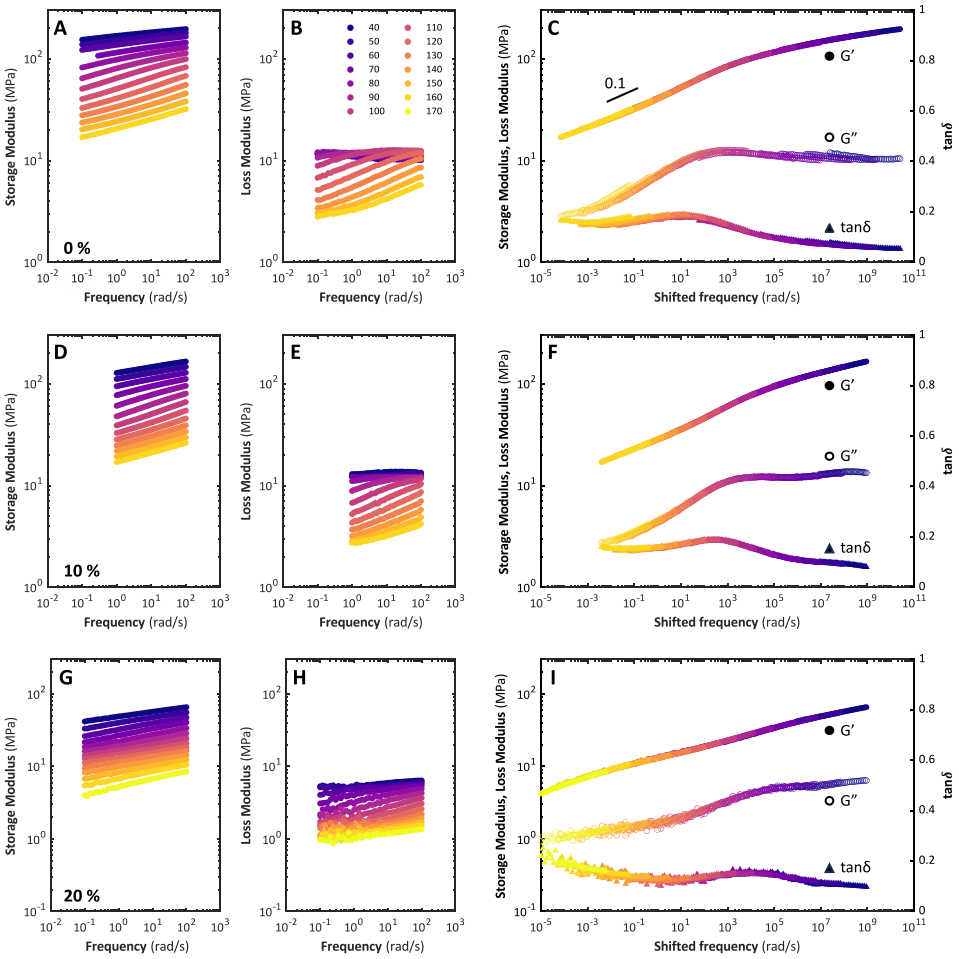

Figure 2. Time temperature superposition (TTS) of complexmer with increasing concentration of ionic liquid (IL-S). (A) The storage modulus (G') and (B) loss modulus (G'') of nonplasticized complexmer are shifted horizontally with respect to a reference temperature (T_{ref}) of 120 °C to form a (C) master curve. Vertical shift factors were not needed. The same is done for the (D−F) complexmer plasticized with 10% IL-S and (G−I) complexmer plasticized with 20% IL-S.

microscope equipped with a white light laser (WLL) and a Becker & Hickl SPC830 time-correlated single photon counting (TCPC) module. The Bodipy rotor fluorophore was excited with a 488 nm laser, emission was captured between 500 and 550 nm through a 10× air objective on a hybrid detector. Acquisition times were typically between 60 and 120 s, images were obtained in a 256 × 256 pixel format. Images were processed in SPCImage 8.5 to generate two-component exponential decay curves for every pixel. FLIM images are presented in a false-color scale that represents the mean fluorescence lifetime.

Fluorescence Recovery after Photobleaching (FRAP). *Sample Preparation.* To prepare the samples for temperature resolved FRAP, complexmer powder was swollen in DMF, which contained fluorescent dye Pyrromethene 546 (0.02−0.03 wt %), and the ionic liquid in different concentrations based on the complexmer mass (20% for IL-S and 35% for IL). These mixtures were stirred overnight, after which the solvent was removed using a rotary evaporator at 60 °C. The FRAP samples were dried in a vacuum oven at 60 °C for at least 3 nights. The complexmers were hot-pressed into thin films using a Specac manual hydraulic press with heated plates between two Teflon sheets. The complexmer powders were heated for 15 min at 160 °C after which 1.5 tons of pressure was applied for 15 min. The samples were then removed from the press and cooled to room temperature.

FRAP Measurements. Temperature resolved FRAP measurements were performed on a Nikon C2 Confocal laser scanning microscope using a 488 nm (15 mW) laser for both measuring and bleaching. The resolution of the images was 512 × 512 px. A disk-shaped Region of Interest (ROI) with a diameter of 30 μm was selected for bleaching at a depth of approximately 10−15 μm. Before the bleaching, 21 images, and after bleaching, 901 images were recorded with a time interval of 2 s at a laser power of 0.15 mW. The bleach consisted of 3 s of 15 mW laser power. The temperature was controlled using a VAHEAT standard Range system from Interherence GmbH in Erlangen. A hot-pressed sample was placed on a smart substrate (SmS) standard range with dimension 18 × 18 × 0.17 (±0.05) mm^3. A Plan Apo 10× (NA = 0.45, WD = 4000 μm) air objective was used with a digital zoom of 4x. FRAP experiments were performed at four temperatures: 25, 50, 75, and 100 °C. Before bleaching, 5 images were recorded, and after bleaching 91 images, with a time interval of 10 s between images.

Analyzing FRAP Data. FRAP data was analyzed using the method of Bos et al.[17] adapted from Taylor et al.[18] The fluorescence in the bleach spot was normalized using

$$\langle C\rangle(t) = \frac{\langle C(r,t)\rangle - \langle C(r,0)\rangle}{\langle C_{\text{prebleach}}\rangle - \langle C(r,0)\rangle} \quad (1)$$

where $\langle C(r,t)\rangle$ is the average intensity of fluorescence in the bleach spot during the measurement, and $\langle C(r,0)\rangle$ is the average intensity of fluorescence in the bleach spot immediately after bleaching. $\langle C_{\text{prebleach}}\rangle$ represents the average intensity in the bleach spot before bleaching. This data was then corrected for changes in background fluorescence during the measurements.

$$C_{\text{cor}}(t) = \langle C(t)\rangle \frac{C_{\text{ref}}(0)}{C_{\text{ref}}(t)} \quad (2)$$

https://doi.org/10.1021/acs.macromol.5c01318
Macromolecules XXXX, XXX, XXX−XXX

where C_{cor} is the corrected intensity concentration. $\langle C \rangle$ is the normalized intensity in the bleach spot. $C_{ref}(0)$ is the intensity in the reference spot far from the bleach spot in the image immediately after bleaching, while $C_{ref}(t)$ is the intensity in the reference spot during the measurement.

Broadband Dielectric Spectroscopy (BDS). Measurements were performed on a Novocontrol BDS Alpha analyzer with Quatro temperature control system. N_2 gas was used for the temperature control. Disk-shaped samples with 10 mm diameter, and 1 mm thickness were used for the experiments. Prior to the experiments, samples were coated with 15 nm of gold using a Q300TD Sputter coater to improve the electrical contact. The samples were mounted between brass electrodes with a diameter of 10 mm. The samples were dried in the sample setup for 1 h at 80 °C. After the drying process, the electrical contact was further tightened ensuring proper electrical contact. The tests were carried out between 10^6−10^{-1} Hz and 160−0 °C at a root-mean-square voltage of 1 V.

RESULTS AND DISCUSSION

Ionic Liquids Plasticize Complexiers without Affecting the Apparent Activation Energy. We apply the Time Temperature Superposition (TTS) principle to complexiers plasticized with ionic liquids (the bulky ionic liquid methyltrioctylammonium bis(trifluoromethylsulfonyl)imide (IL-S) and the smaller ethyl-dimethylpropylammonium bis(trifluoromethylsulfonyl)imide (IL)). Here, we focus on ionic liquid concentrations that give a T_g that is low enough to capture the full thermal transition (Table S1). The TTS principle is based on the idea that increasing the temperature of a material has a similar effect as reducing the time over which it is deformed.[19] This occurs because the different relaxation times associated with a particular relaxation process share the same temperature dependence.[20] Using this principle, we can probe the material's mechanical response at time scales that are otherwise inaccessible, either due to instrument limitations or experiment duration limitations.[21] To this end, we measure a series of frequency sweeps at a range of temperatures for screened polystyrene complexiemer (Figure 1) samples plasticized with 0%, 10% and 20% screened ionic liquid IL-S (Figure 1), which is a bulky ionic liquid that resembles the chemical structure of the complexiemer. The storage and loss moduli, reported in Figure 2A-B, D-E and G-H, show an overall decrease with increasing temperature, indicating a temperature-induced softening of the material. Yet, at all explored temperatures, the complexiemers remain solid, as the storage moduli are always larger than the loss moduli. The $\tan\delta$ $\left(\tan\delta = \frac{G''}{G'}\right)$ values, represented in Figure S2 are thus always <1 in the employed frequency range. We verify the rheological simplicity of the samples by constructing Van Gurp-Palmen plots,[22] plotting the phase shift as a function of the complex modulus (Figure S3). These curves are expected to merge onto a single line when TTS is applicable; we note that TTS holds well for most samples, though deviate somewhat from rheological simplicity with high ionic liquid concentrations. Master curves are constructed from these data by shifting the curves horizontally relative to a reference temperature of 120 °C by multiplying the frequency axis with only a temperature-dependent shift factor a_T (Figure 2C, F and I respectively), no vertical shift factors were used. This shifting gives access to the relaxation spectrum over more than ten decades of frequency. The resulting relaxation spectra appear notably broad, with extended power law regimes at low frequencies, with slopes of approximately 0.1. We observe a shift in the dynamic glass transition, which can be identified by the peaks, here the very broad shoulders, in the loss modulus and tanδ master curves. Ionic liquids clearly lower the glass transition temperature (T_g), also known as the α transition,[23,24] as these features shift to higher frequencies. This aligns with our findings on the T_g of these systems, as measured from temperature sweeps, presented in our previous work[9] Table S1 and Figure S4.

When shifting TTS master curves with different plasticizers and plasticizer content onto one single master curve relative to the nonplasticized complexiemer, we can identify a time−temperature-plasticizer superposition (Figure 3). In case of plasticizing the complexiemer with (small amounts) of plasticizers IL-S and a neutral plasticizer dioctyl phthalate (DOP), the dynamical relaxation mechanisms are not fundamentally changed but accelerated by orders of magnitude, as shown in the shift factors (Figure 3, caption), as they collapse on the same master curve. A larger amount (35%) of a nonscreened, small molecule plasticizer IL (Figure 1) leads to deviations from this master curve, likely by changing the relaxation mechanism. In our previous work, SAXS analysis revealed that this concentration of IL alters the network structure,[9] potentially accounting for the differences in relaxation.

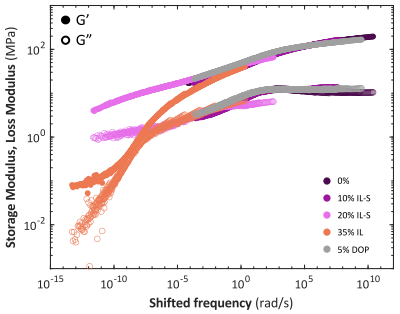

Figure 3. Time−temperature-plasticizer superposition of plasticized complexiemers. The master curves are shifted along the frequency axis relative to the 0% data until the largest portion of the curves overlap, forming a single master curve.. The respective shift factors for 10% IL-S, 20% IL-S, 35% IL, and 5% DOP were 0.05, 4×10^{-7}, 1×10^{-10}, and 0.7.

Above T_g, strong glass-forming materials such as silica glass[25] and "vitrimers"[15,26]—dynamic polymer networks that can undergo bond exchange reactions—show a gradual trend in the relaxation time (which scales with the shift factor a_T), characterized by a constant activation energy that complies with the Arrhenius law:

$$\ln(a_T) = \ln(A) + \frac{E_a}{R}\cdot\frac{1}{T} \tag{3}$$

where A is the pre-exponential factor, E_a the activation energy in J/mol and R the gas constant. Most glassy polymers deviate strongly from this trend and show a much steeper decrease in the relaxation time above T_g, which can be described empirically by the Williams−Landel−Ferry (WLF) model:[27,28]

$$\log(a_T) = -\frac{C_1(T - T_{ref})}{C_2 + (T - T_{ref})} \tag{4}$$

where C_1 and C_2 are constants, and T_{ref} is the reference temperature with respect to which the curves are shifted. We observe in Figure 4 that IL-S plasticized complexiemers in fact

https://doi.org/10.1021/acs.macromol.5c01318
Macromolecules XXXX, XXX, XXX−XXX

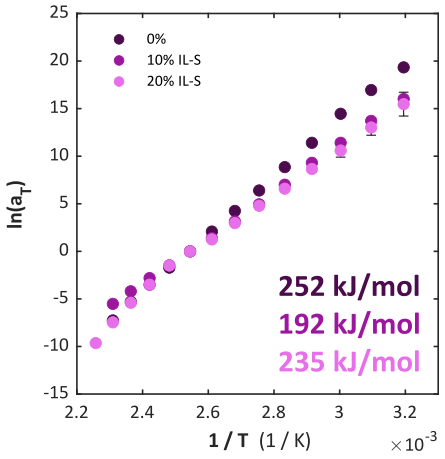

Figure 4. Arrhenius plots and activation energies of complexiners with 0% IL-S, 10% IL-S, and 20% IL-S. All three samples follow the Arrhenius law and have similar activation energies. All shift factors were determined relative to a reference temperature of 120 °C.

follow an Arrhenius law over the entire temperature window, thus exhibiting behavior similar to that of vitrimers. The activation energies of the plasticized samples are slightly lower than the nonplasticized one, but do not decrease further upon adding more ionic liquid. Plasticization with 35% of a nonscreened ionic liquid IL again leads to a small decrease of the activation energy (Figure S6), even though the moduli are much more strongly affected, as shown in our previous work.[9] Finally, plasticization with 5% of a nonionic plasticizer DOP also leads to a similar activation energy (Figure S7). We note that accurate determination of shift factors - and therefore activation energies - is challenging at temperatures below T_g. For the samples where this is possible, we have therefore determined the activation energies using data above T_g only. For the pure complexiner, where T_g is too high, we report an activation energy using data below T_g. We note, however, that for the samples with lower T_g differences in apparent activation energy below and above T_g are modest. All activation energies found are in the range of 200−250 kJ/mol, which is very high compared to the theoretically expected bond energy of an ionic bond according to Coulomb's Law, which is in the order of 50 kJ/mol (Note S1). In Note S2, we explain how the "apparent activation energy" can be significantly higher than the true E_a when E_a itself depends on temperature,[29] which may be the case here, and also demonstrate that when E_a varies linearly

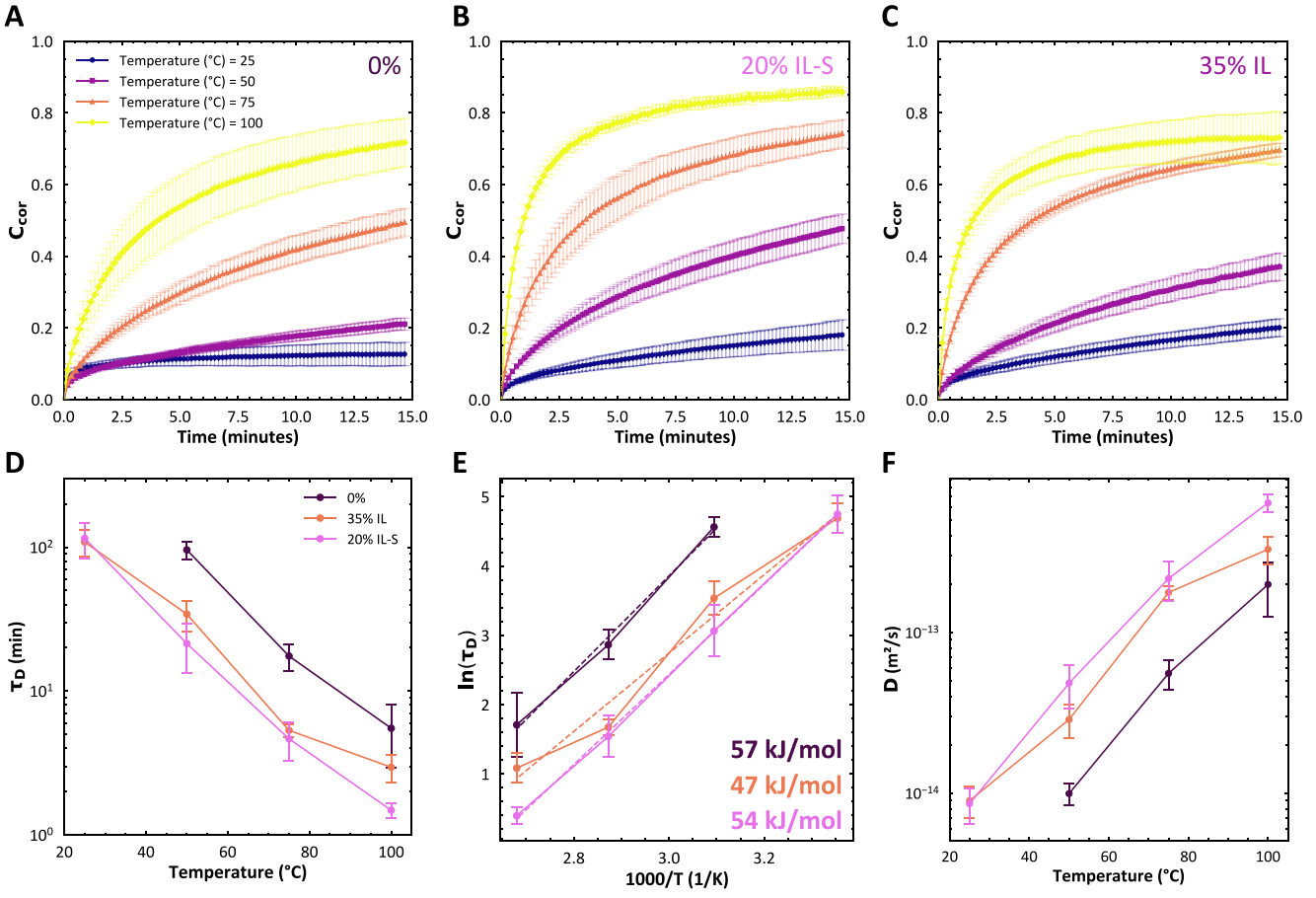

Figure 5. The fluorescence recovery after photobleaching of complexiners at elevated temperatures. The intensity was corrected with respect to a reference spot. The corrected intensity (C_{cor}) was here plotted as a function of time for (A) 0% IL-S, (B) 20% IL-S, and (C) 35% IL. The errors are represented by the shaded areas. In all cases, the recovery is accelerated with increasing temperature. The recovery curves were fitted with a 2D diffusion model for a disk-shaped bleach spot. (D) The characteristic relaxation time τ_D of the diffusion model as a function of temperature shows a decrease in the relaxation time with temperature. Ionic liquid plasticizers speed up the relaxation. (E) The Arrhenius plot shows that the relaxation times roughly follow an Arrhenius law with activation energies around 50 kJ/mol. (F) The diffusion coefficients were calculated from the diffusion times using eq 6.

https://doi.org/10.1021/acs.macromol.5c01318
Macromolecules XXXX, XXX, XXX−XXX

with T, the Arrhenius plot remains a straight line. Clearly, all plasticizers accelerate the relaxation, but with small impact on its temperature dependence. This behavior is particularly noteworthy given that ionic plasticizers in hydrated polyelectrolyte complexes typically reduce the activation energy more strongly,[30,31] suggesting a different mechanism is at play here.

Ionic Liquids Enhance the Diffusion of Small Molecules in Compleximers. With rheometry, macroscopic relaxation of the material as a whole is probed. Using rheological TTS we find activation energies for structural relaxation to be much higher than those expected for the molecular relaxation of ionic supramolecular interactions. This could suggest that in rheometry collective relaxations taking place at larger length scales are probed. To investigate the material dynamics at smaller length scales, where collective effects are expected to be smaller, we study the diffusion of small molecules in the polymer matrix, using fluorescence recovery after photobleaching (FRAP). This method is typically used to investigate diffusion in biological cells,[32] but has also been used to study mobility in polyelectrolyte multilayers.[33,34] For this technique, we incorporate a fluorescent dye, Pyrromethene 546, in addition to plasticizers, in complexime films which we investigate under the confocal microscope. The diffusion of the fluorescent dye in a polymer matrix can be interpreted using theories based on free volume. The thermal expansion of the material leads to an increase in free volume and a concomitant increase of the diffusion coefficient.[35,36] We bleach a disk-shaped region of interest (ROI) in the complexime, and study the recovery of the fluorescence intensity, resulting from diffusive processes, as a function of time. Due to diffusive mixing, unbleached fluorophores mix with the bleached fluorophores in the bleach spot, leading to an increase of fluorescence over time. As the acquisition of the images used to map recovery can also induce mild bleaching, we correct for this by recording background intensities in each frame (Figure S8). We measure the recovery at four temperatures: 25, 50, 75, and 100 °C for S compleximers with 0% ionic liquid (Figure S9), 20% IL-S (Figure S10) and 35% IL (Figure S11). We measure at least 8 different spots per temperature for each of the samples, and plot the average recovery curves in Figure 5A−C.

The fluorescence recovery is generally accelerated with increasing temperature. At 25 °C, the initial recovery is relatively fast, which may be due to temporary heating of the sample as a result of the high-intensity laser. We also show through plotting the corrected recovery at a fixed time point, 10 min, as a function of temperature, that the recovery is accelerated with temperature and with the addition of ionic liquid. The screened ionic liquid IL-S, which has a bulkier cation, is slightly more effective than the nonscreened IL (Figure S12).

The more subtle effects of temperature and plasticizer content can be more effectively quantified by fitting the individual recovery curves with a diffusion model for disk-shaped ROIs:[37,38]

$$f(t) = \exp\left(-\frac{2\tau_D}{t}\right)\left[I_0\left(\frac{2\tau_D}{t}\right) + I_1\left(\frac{2\tau_D}{t}\right)\right] \quad (5)$$

where I_0 and I_1 are modified Bessel functions of the first kind, τ_D is the characteristic diffusion time and the maximum recovery is set to 1. The diffusion coefficient D can be calculated through

$$\tau_D = \frac{r^2}{4D} \quad (6)$$

with r the radius of the photobleached area. Despite having only one fitting parameter, the model fits the recovery data well, except for the nonplasticized complexime at 25 °C, where the heating of the sample during bleaching interferes with the recovery process. For all other samples, we find that the characteristic diffusion time τ_D decreases with increasing temperature, but also that the addition of plasticizer overall lowers τ_D somewhat (Figure 5D). This means that the ionic liquid makes the polymer matrix more mobile or that the fluorescent dye can diffuse through the ionic liquid to the bleached spot. The Arrhenius plot of the FRAP diffusion times gives activation energies around 50 kJ/mol for the plasticized samples, much smaller than found from the rheology data (Figure 5E). This suggests that the relaxation of the matrix at the molecular scale, as probed through small molecule diffusion, is governed by a different processes than that found in the macroscopic rheology experiments above. An overview of the relaxation times of the various samples is reported in Table S2. The corresponding diffusion coefficients D are roughly between 10^{-14} and 10^{-12} m^2/s (Figure 5F). These diffusion coefficients are relatively high compared to those for, for example, small molecules in PMMA in the vicinity of T_g.[39] This suggests that the free volume is larger in our compleximers than that in traditional thermoplastics.

Plasticized Compleximers Are Heterogeneous. Given that the macroscopic and molecular measurements of material dynamics suggest that different processes influence relaxation at different length scales, we asked the question about the spatial organization of the material. Are the polymer and plasticizer homogeneously distributed throughout the material, or are there distinct spatial heterogeneities that could explain the length-scale dependent relaxation? Here we map the spatial distribution of material dynamics using molecular rotor dyes: a class of fluorescent dyes whose fluorescence lifetime is sensitive to the degree of free volume in their immediate surroundings.[16] Using Fluorescence Lifetime Imaging (FLIM), this gives access to free volume maps of the material at confocal (∼200 nm) resolution. In low-viscosity environments, or when the environment allows free rotation, this dye loses its energy through nonradiative processes (without emitting light), leading to a short fluorescence lifetime. In more viscous environments, or when rotation is hindered, the dye releases the energy via fluorescence (light emission), resulting in a longer lifetime.[40] We here make complexime films with both rotor dye and ionic liquid incorporated in a range of concentrations and measure the fluorescence lifetimes at room temperature (Figure 6A for the unplasticized material, B−D for the IL plasticizer and E−G for the IL-S plasticizer). Note that the films fragmented upon transferring them from the hot press to the microscope slide, so that these measurements were done on flakes of complexime samples, rather than on bulk films. We can nevertheless interpret these data qualitatively, and observe that compleximers are highly heterogeneous; the lifetimes vary from region to region within a single flake. Distinguishing whether the heterogeneity arises from intrinsic variations in the material or from an uneven distribution of the ionic liquid is challenging and we note that the sample with 0% plasticizer also shows considerable

https://doi.org/10.1021/acs.macromol.5c01318
Macromolecules XXXX, XXX, XXX−XXX

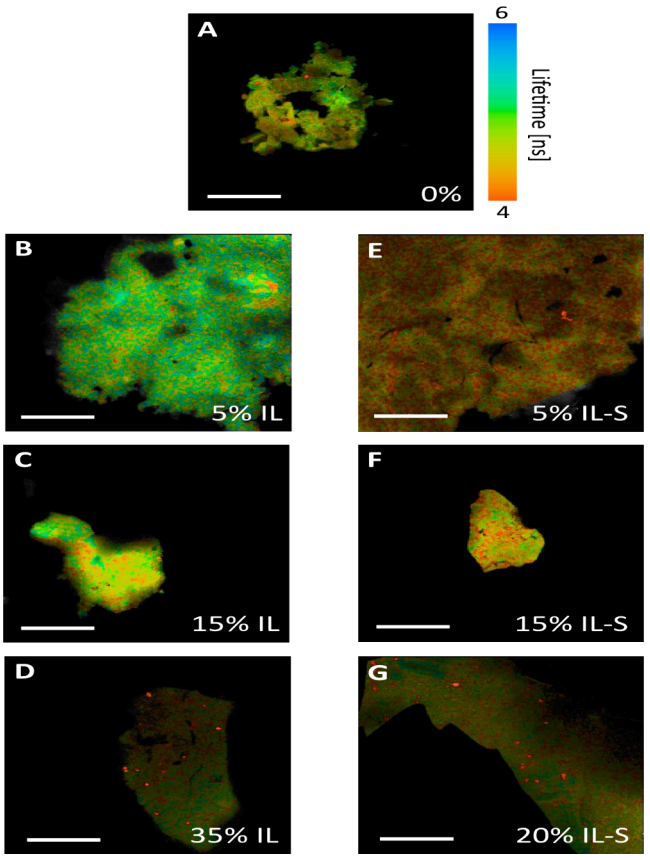

Figure 6. Plasticized complexiers are heterogeneous. We investigate the spatial distribution of the fluorescence lifetime using fluorescence lifetime imaging (FLIM) for complexiers flakes with (A) 0% plasticizer, with (B−D) 5, 15, and 35% IL, and with (E−G) 5, 15, and 20% IL-S. All scale bars are 300 μm. In the color bar, long lifetimes are represented in blue and short lifetimes are represented in red.

heterogeneity. However, the well-defined red spots in samples with high plasticizer content suggest the presence of domains with shorter lifetimes and, consequently, lower viscosity. These domains may represent droplets of ionic liquid that are not fully integrated into the polymer matrix. Indeed, SAXS measurements carried out previously showed a slight modulation of the scattering curve at these high ionic liquid contents, suggesting the formation of phase-separated domains.[9] The effect of the ionic liquid content on the fluorescence lifetime and heterogeneity is not obvious from the images. We plot histograms describing the lifetime distribution in Figure S13 and find that although there is no conclusive trend in the average lifetime with increasing plasticizer content, the lowest lifetimes are better represented in samples with high plasticizer content (35% IL and 20% IL-S).

Dielectric Relaxations in Complexiers. Since rheology and FRAP reveal markedly different activation energies due to their length-scale-dependent relaxation mechanisms, we employ broadband dielectric spectroscopy (BDS) to investigate relaxation spectra across an extensive frequency range. This approach enables the characterization of relaxations spanning a broad spectrum of length and time scales. It probes the movement of electronic dipoles resulting from an applied electric field.[41] From dielectric experiments, we measure conductivity effects and dipole relaxation processes. Besides the α relaxation, which is a slow relaxation resulting from the cooperative movement of large segments of the polymer chains, such as the backbone or entire chain segments,[42] ionic materials can exhibit an α_2 relaxation. This α_2 relaxation is found in ionomers—materials where ionic groups form clusters that restrict the mobility of the chains—showing a delayed stress relaxation.[43] The dissociation and association of ions, or so-called "ion hopping" activates a dielectric "α_2" process that is related to the association energy of the ionic group.[44,45] BDS measurements of plasticized ionomers generally display an increase in the conductivity while preserving the ion transport mechanism.[46]

We perform BDS experiments on samples with 0, 10 and 20% IL-S and investigate the real part (ε') and the imaginary part (ε'') of the dielectric permittivity. The real component, ε' (Figure S14A, D, G), represents the material's ability to store electrical energy by polarizing in response to the applied field.[47] This is often influenced by dipolar orientation within the material and changes with ionic content and molecular structure.[48] The imaginary component, ε'' (Figure S14B, E, H), relates to the energy dissipated as heat due to relaxation and conduction processes within the material.[41] Since ε'' is susceptible to electrode polarization effects, we derive ε''_{KK} from ε' through the Kramers−Kronig transformation, which better highlights the material relaxation effects[41,49] (Figure S14C, F, I), following:

$$\varepsilon''_{KK} = -\frac{\pi}{2}\frac{\partial \varepsilon'}{\partial \ln(\omega)} \tag{7}$$

Similar to the rheological frequency sweeps, we then apply the time temperature superposition (TTS) principle to the BDS data by shifting ε' and ε_{KK}'' horizontally over the frequency axis by multiplying it with a temperature dependent shift factor a_T (Figure 7A−C for the real part and D−F for the imaginary part) with the same T_{ref} of 120 °C. These master curves show a contribution of the conductivity at low frequencies (dotted line), and a dipole relaxation at higher frequencies in the form of a broad peak or shoulder (dashed line), which shifts to higher frequencies with increasing ionic liquid concentration. These peaks are found at similar frequencies as the loss peak in the respective rheological TTS master curves (Figure 2). The fact that the permittivities collapse so well on a master curve indicates that both the conductivity and relaxation depend on temperature in the same way. The Arrhenius plot of the shift factors shows an Arrhenius dependence, with activation energies around 110 kJ/mol, displaying a very slight decrease with increasing plasticizer content (Figure 7 insets). The magnitude of the activation energies is in between those found with rheology and FRAP.

The ε''_{KK} master curves (Figure 7) were fitted with a conductivity term at low frequencies and the Havriliak−Negami model at high frequencies. The conductivity term is described by

$$\varepsilon''(\omega) = \left(\frac{\sigma_{DC}}{\varepsilon_0 \omega}\right)^n \tag{8}$$

where σ_{DC} is the direct current (DC) conductivity of the material.[41,48,50] It indicates how easily an electric current can flow through the material under a steady-state electric field. The DC conductivity can be influenced by factors such as temperature, ion mobility, and the concentration of charge carriers.[51] σ_{DC} increases with almost 2 orders of magnitude with increasing plasticizer content (Figure 8A), indicating a

https://doi.org/10.1021/acs.macromol.5c01318
Macromolecules XXXX, XXX, XXX−XXX

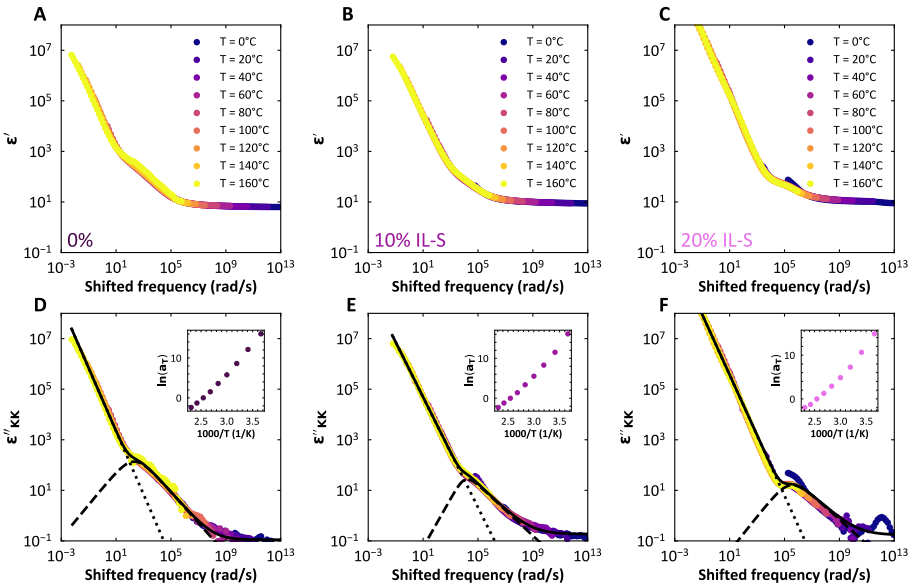

Figure 7. BDS master curves of complexiers plasticized with IL-S. (A, B, C), Master curve of the real part of the dielectric permittivity ε' of S complexiemer with 0%, 10%, and 20% IL-S, respectively, obtained after time−temperature superposition (TTS) with a reference temperature of 120 °C. (D, E, F), Master curve of the imaginary part of the dielectric permittivity, found through transforming ε' using the Kramers−Kronig transformation. The master curves were fitted with a conductivity term (dotted line) and the Hraviliak−Nagami model (dashed line); the full fit is shown as a black line. The insets show the Arrhenius plots of the temperature dependent shift factors α_T of the TTS shifting of ε_{KK}'' at different concentrations of ionic liquid, and the respective activation energies are 114, 83, and 78 kJ/mol. Also here, vertical shift factors were not needed.

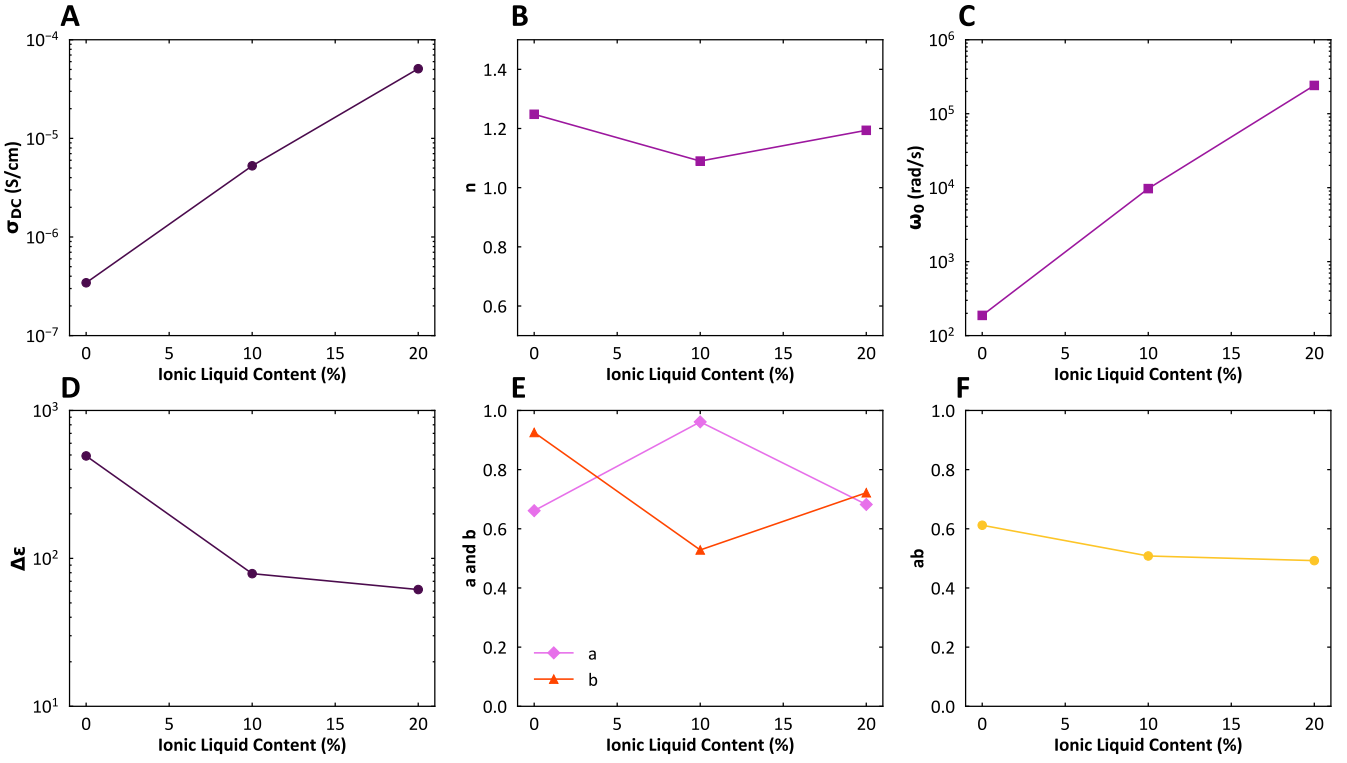

Figure 8. Fitting parameters of the conductivity model and Havriliak−Negami (HN) model at different ionic liquid (IL-S) concentrations. (A) σ_{DC}, the direct current (DC) conductivity at $T_r ef$ = 120 °C increases with ionic liquid. (B) $n \approx 1$ which means we mostly measure conductivity effects. (C) The characteristic relaxation frequency ω_0 increases with plasticizer content, (D) $\Delta\varepsilon$, which relates to the dielectric constant, decreases. (E) a and b, which dictate the broadening and asymmetry of the relaxation peak, are similar. (F) The product of a and b is approximately 0.5.

strong increase in ion mobility. Ionic liquids have a much higher mobility than the polymers since the ions are much smaller. We also plot n, which describes the frequency dependence of the imaginary part of the permittivity in the low frequency regime (Figure 8B).[52] For pure Ohmic conductivity, n = 1, but the exponent may deviate due to interference of electrode polarization effects that can also show up at low frequencies. Electrode polarization is the

https://doi.org/10.1021/acs.macromol.5c01318
Macromolecules XXXX, XXX, XXX−XXX

accumulation of charges at the electrode. We here find that this coefficient is generally only slightly larger than 1, which means we mostly measure conductivity.[52]

At higher frequencies we use the Havriliak–Negami[53] model to fit the dielectric (segmental) relaxations:

$$\epsilon''_{HN}(\omega) = \mathrm{Im}\left\{\frac{\Delta\varepsilon}{\left[1 + \left(\frac{i\omega}{\omega_0}\right)^a\right]^b}\right\} \quad (9)$$

The HN model is an (empirical) generalization of the Debye model for dipole relaxation to a broader distribution of relaxation times.[41,54] This model is used to approximate the stretched exponential decay of the ε''. The parameters a and b respectively provide the broadening and asymmetry of the relaxation spectrum,[55] where broadening is thought to be caused by dynamic heterogeneity.[41] The peaks in the HN fits, captured by the characteristic relaxation frequency ω_0, shift to higher frequencies with increasing temperature (Figure 8C), signifying an acceleration of the segmental motion.[56] We also plot $\Delta\varepsilon$, which represents the change in permittivity (dielectric constant) of the material (Figure 8D). $\Delta\varepsilon$ decreases with increasing ionic liquid plasticization. Since this parameter is related to the strength of the relaxation,[57] we speculate that ionic liquids weaken the dipoles by being close to the ion pairs. The parameters a and b obtained from the fits are shown in Figure 8E. However, we note that a and b are difficult to fit individually since the left side of the relaxation is overshadowed by the conductivity term. The product of a and b obtained from the fits is more robust, as it is equal to the slope on the right side of the relaxation peak. This product is approximately the same for all three plasticizer contents and equal to 0.5 (Figure 8F). This may indicate that the underlying relaxation mechanisms are not affected by the ionic liquid, only accelerated. This can also be observed from Figure 7: ω_0 and σ_{DC} increase with increasing temperature, but the parameters $\Delta\varepsilon$, a, b, and n do not, as the shapes of the curves stay the same.

CONCLUSIONS

In nature, polyelectrolyte complexes and complex coacervates such as biological adhesives and slimes typically contain hydration water and counterions, which plasticize the material. In contrast, compleximers, which are not plasticized by default, can be plasticized on demand by incorporating ionic liquids that resemble the chemical structure of the compleximer ions. While it is evident that ionic liquids effectively plasticize compleximers by lowering their T_g, it has remained unclear how these plasticizers affect the material dynamics. In this study, we investigated the relaxation dynamics of compleximers plasticized with varying concentrations of two types of ionic liquids: methyl-trioctylammonium bis(trifluoromethylsulfonyl)imide (IL-S) and ethyldimethylpropylammonium bis(trifluoromethylsulfonyl)imide (IL). To probe different length scales—from the bulk material to individual ionic segments—we employed a combination of rheological time–temperature superposition (TTS), fluorescence recovery after photobleaching (FRAP), and broadband dielectric spectroscopy (BDS) combined with TTS.

Our findings demonstrate that ionic liquids effectively lower the glass transition temperature and modulus of compleximers while enhancing diffusion processes and segmental motion. Notably, the temperature dependence of these processes is not significantly affected, as the presence or concentration of ionic liquid decreases the apparent activation energy only slightly across the samples. This sets compleximer plasticization apart from conventional materials, including PECs, where the addition of a plasticizer typically results in a stronger decrease in activation energy.[30,31,58−60] For moderately plasticized compleximers, we can identify a time–temperature-plasticizer superposition through rheological TTS. Deviations from this master curve were found when plasticizing with 35% IL, a small molecule ionic liquid, in which we also found a change in structure using SAXS.[9] The addition of IL-S, which more closely resembles the bulkiness and chemistry of the compleximer, instead has a similar relaxation mechanism as the non plasticized compleximer. Adding neutral plasticizers dioctyl phthalate in small concentrations (5%) plasticizes compleximers, but increasing the concentration leads to phase separation[9]).

The relaxation of all compleximer samples follows the Arrhenius relation rather well, which implies that they classify as "strong glass formers", similarly to vitrimers.[15,26] However, the apparent activation energy of compleximers as measured with rheology is significantly higher than that of vitrimers. While the precise origin of this high activation energy is not clear, we speculate that it is due to the nature of the bonds in the material. Vitrimer relaxation is governed by exchange of dynamic covalent bonds, with a well-defined bond energy. Compleximers, by contrast, are held together by noncovalent and long-ranged ionic bonds. Upon increasing the temperature, thermal expansion of the material may thus increase the distance between the charges, thereby leading to a gradual weakening of the ionic interactions and a decrease of the activation energy. As shown previously[29] and explained in Note S2, such a temperature-dependent activation energy can significantly increase the apparent activation energy measured with rheology.

It is important to note that the apparent activation energy derived from rheological measurements (approximately 200–250 kJ/mol) is substantially higher than that obtained from the other techniques, around 90 kJ/mol for BDS and 50 kJ/mol for FRAP (Table S2). Since the different techniques give different activation energies, this suggests they probe different relaxation processes. BDS is sensitive to the dynamics and reorientation of dipoles and ion pairs, which is governed mostly by localized segmental motions. By contrast, rheology probes viscoelastic relaxations that involve cooperative chain motion over longer length scales and reorganization of multiple ion pairs. Such cooperative motions have been shown to depend more strongly on temperature, therefore leading to a larger apparent activation energy.[61−63] The FRAP measurements probe the diffusive motion of a neutral dye molecule in the material. This motion depends on the free volume in the material, which increases with temperature as a result of thermal expansion. However, it is probably not strongly influenced by the ionic bonds directly, which could explain the lower apparent activation energy measured with FRAP.

Despite the fact that ionic liquids have only a small effect on the activation energies, we do find they decrease the modulus at elevated temperature, decrease the glass transition temperature, accelerate the diffusion of a fluorescent dye through the polymer matrix and increase segmental motion. This means that the pre-exponential factor A (eq 3) is affected by the ionic

https://doi.org/10.1021/acs.macromol.5c01318
Macromolecules XXXX, XXX, XXX−XXX

liquid. This opens up intriguing possibilities to explore the distinct mechanisms at play in compleximers, offering new insights into their unique plasticization behavior. Through fluorescence lifetime imaging, we also find that compleximers are heterogeneous, meaning that ionic liquids may not be evenly dispersed throughout the system. We will further investigate the effect of added plasticizers, their distribution, and their influence on the relaxation dynamics and compleximer structure using molecular dynamics simulations. Additionally, it would be interesting to develop new types of compleximers, with a more flexible backbone chemistry, that can show the full thermal transition without the need of extrinsic plasticization, allowing for the characterization of pure compleximer relaxations.

■ ASSOCIATED CONTENT

Supporting Information

The Supporting Information is available free of charge at https://pubs.acs.org/doi/10.1021/acs.macromol.5c01318.

Additional explanatary notes; additional rheological measurements; FRAP data; fluorescence lifetime distributions; dielectric spectroscopy data; tables with glass transition temperatures and apparent activation energies (PDF)

■ AUTHOR INFORMATION

Corresponding Authors

Sophie G. M. van Lange − *Physical Chemistry and Soft Matter, Wageningen University and Research, 6708 WE Wageningen, The Netherlands;* orcid.org/0009-0007-5826-3224; Email: sophie.vanlange@wur.nl

Jasper van der Gucht − *Physical Chemistry and Soft Matter, Wageningen University and Research, 6708 WE Wageningen, The Netherlands;* orcid.org/0000-0001-5525-8322; Email: jasper.vandergucht@wur.nl

Authors

Riccardo Biella − *Department of Aerospace Structures and Materials, Faculty of Aerospace Engineering, Delft University of Technology, 2629 HS Delft, The Netherlands*

Diane W. te Brake − *Physical Chemistry and Soft Matter, Wageningen University and Research, 6708 WE Wageningen, The Netherlands*

Sinty Dol − *Physical Chemistry and Soft Matter, Wageningen University and Research, 6708 WE Wageningen, The Netherlands*

Maarten Besten − *Laboratory of Biochemistry, Wageningen University and Research, 6708 WE Wageningen, The Netherlands;* orcid.org/0000-0001-5823-2320

Joris Sprakel − *Laboratory of Biochemistry, Wageningen University and Research, 6708 WE Wageningen, The Netherlands;* orcid.org/0000-0001-6532-4514

Santiago J. Garcia − *Department of Aerospace Structures and Materials, Faculty of Aerospace Engineering, Delft University of Technology, 2629 HS Delft, The Netherlands;* orcid.org/0000-0002-2211-9972

Complete contact information is available at: https://pubs.acs.org/10.1021/acs.macromol.5c01318

Notes

The authors declare no competing financial interest.

■ ACKNOWLEDGMENTS

This work was supported by the Dutch Research Council (NWO) OCENW.KLEIN.326. (J.v.d.G.).

■ REFERENCES

(1) Hofman, A. H.; van Hees, I. A.; Yang, J.; Kamperman, M. Bioinspired underwater adhesives by using the supramolecular toolbox. *Advanced Materials* **2018**, *30*, 1704640.

(2) Baer, A.; Hänsch, S.; Mayer, G.; Harrington, M. J.; Schmidt, S. Reversible supramolecular assembly of velvet worm adhesive fibers via electrostatic interactions of charged phosphoproteins. *Biomacromolecules* **2018**, *19*, 4034−4043.

(3) Aumiller, W. M., Jr; Pir Cakmak, F.; Davis, B. W.; Keating, C. D. RNA-based coacervates as a model for membraneless organelles: formation, properties, and interfacial liposome assembly. *Langmuir* **2016**, *32*, 10042−10053.

(4) Meka, V. S.; Sing, M. K.; Pichika, M. R.; Nali, S. R.; Kolapalli, V. R.; Kesharwani, P. A comprehensive review on polyelectrolyte complexes. *Drug Discovery Today* **2017**, *22*, 1697−1706.

(5) Wang, Q.; Schlenoff, J. B. The Polyelectrolyte Complex/Coacervate Continuum. *Macromolecules* **2014**, *47*, 3108−3116.

(6) Suarez-Martinez, P.; Batys, P.; Sammalkorpi, M.; Lutkenhaus, J. Time−Temperature and Time−Water Superposition Principles Applied to Poly(allylamine)/Poly(acrylic acid) Complexes. *Macromolecules* **2019**, *52*, 3066−3074.

(7) Syed, V. M. S.; Srivastava, S. Time−Ionic Strength Superposition: A Unified Description of Chain Relaxation Dynamics in Polyelectrolyte Complexes. *ACS Macro Lett.* **2020**, *9*, 1067−1073. PMID: 35648617.

(8) Zhang, Y.; Batys, P.; O'Neal, J. T.; Li, F.; Sammalkorpi, M.; Lutkenhaus, J. L. Molecular Origin of the Glass Transition in Polyelectrolyte Assemblies. *ACS Central Science* **2018**, *4*, 638−644.

(9) van Lange, S. G. M.; Te Brake, D. W.; Portale, G.; Palanisamy, A.; Sprakel, J.; van der Gucht, J. Moderated ionic bonding for water-free recyclable polyelectrolyte complex materials. *Science Advances* **2024**, *10*, eadi3606.

(10) Lei, Z.; Chen, B.; Koo, Y.-M.; MacFarlane, D. R. Introduction: ionic liquids. *Chem. Rev.* **2017**, *117*, 6633.

(11) Cadogan, D. F.; Howick, C. J. *Ullmann's Encyclopedia of Industrial Chemistry*; John Wiley & Sons, Ltd., 2000.

(12) Lalwani, S. M.; Batys, P.; Sammalkorpi, M.; Lutkenhaus, J. L. Relaxation Times of Solid-like Polyelectrolyte Complexes of Varying pH and Water Content. *Macromolecules* **2021**, *54*, 7765−7776.

(13) Spruijt, E.; Sprakel, J.; Lemmers, M.; Stuart, M. A. C.; van der Gucht, J. Relaxation Dynamics at Different Time Scales in Electrostatic Complexes: Time-Salt Superposition. *Phys. Rev. Lett.* **2010**, *105*, 208301.

(14) Spruijt, E.; Cohen Stuart, M. A.; van der Gucht, J. Linear Viscoelasticity of Polyelectrolyte Complex Coacervates. *Macromolecules* **2013**, *46*, 1633−1641.

(15) Montarnal, D.; Capelot, M.; Tournilhac, F.; Leibler, L. Silica-like malleable materials from permanent organic networks. *Science* **2011**, *334*, 965−968.

(16) Besten, M.; Hendriksz, M.; Michels, L.; Charrier, B.; Smakowska-Luzan, E.; Weijers, D.; Borst, J. W.; Sprakel, J. CarboTag: a modular approach for live and functional imaging of plant cell walls. *Nat. Methods* **2025**, *22*, 1081.

(17) Bos, I.; Brink, E.; Michels, L.; Sprakel, J. DNA dynamics in complex coacervate droplets and micelles. *Soft Matter* **2022**, *18*, 2012−2027.

(18) Taylor, N. O.; Wei, M.-T.; Stone, H. A.; Brangwynne, C. P. Quantifying dynamics in phase-separated condensates using fluorescence recovery after photobleaching. *Biophysical journal* **2019**, *117*, 1285−1300.

(19) Urzhumtsev, Y. S. Time-temperature superposition. Review. *Polymer Mechanics* **1976**, *11*, 57−72.

(20) Van Gurp, M.; Palmen, J. Time-temperature superposition for polymeric blends. *Rheol. Bull.* **1998**, *67*, 5−8.

(21) Sokolov, A.; Hayashi, Y. Breakdown of time−temperature superposition: From experiment to the coupling model and beyond. *Journal of non-crystalline solids* **2007**, *353*, 3838−3844.
(22) Trinkle, S.; Friedrich, C. Van Gurp-Palmen-plot: a way to characterize polydispersity of linear polymers. *Rheol. Acta* **2001**, *40*, 322−328.
(23) Kendall, M. J.; Siviour, C. R. Rate dependence of poly (vinyl chloride), the effects of plasticizer and time−temperature superposition. *Proceedings of the Royal Society A: Mathematical, Physical and Engineering Sciences* **2014**, *470*, 20140012.
(24) Soong, S. Y.; Cohen, R. E.; Boyce, M. C.; Mulliken, A. D. Rate-Dependent Deformation Behavior of POSS-Filled and Plasticized Poly(vinyl chloride). *Macromolecules* **2006**, *39*, 2900−2908.
(25) Angell, C. A. Formation of glasses from liquids and biopolymers. *Science* **1995**, *267*, 1924−1935.
(26) Denissen, W.; Winne, J. M.; Du Prez, F. E. Vitrimers: permanent organic networks with glass-like fluidity. *Chemical science* **2016**, *7*, 30−38.
(27) Li, R. Time-temperature superposition method for glass transition temperature of plastic materials. *Materials Science and Engineering: A* **2000**, *278*, 36−45.
(28) Ljubić, D.; Stamenović, M.; Smithson, C.; Nujkić, M.; Medo, B.; Putić, S. Time: Temperature superposition principle: Application of WLF equation in polymer analysis and composites. *Zastita Materijala* **2014**, *55*, 395−400.
(29) Struik, L. The apparent activation energy for mechanical and dielectric relaxation in glass-forming (polymeric) liquids: A misconception? *Polymer* **1997**, *38*, 733−735.
(30) Spruijt, E.; Sprakel, J.; Lemmers, M.; Stuart, M. A. C.; Van Der Gucht, J. Relaxation Dynamics at Different Time Scales in Electrostatic Complexes:<? format?> Time-Salt Superposition. *Physical review letters* **2010**, *105*, 208301.
(31) Ali, S.; Prabhu, V. M. Relaxation Behavior by Time-Salt and Time-Temperature Superpositions of Polyelectrolyte Complexes from Coacervate to Precipitate. *Gels* **2018**, *4*, 11.
(32) Houtsmuller, A. B. Fluorescence recovery after photobleaching: application to nuclear proteins. In *Microscopy Techniques*; Advances in Biochemical Engineering, Vol. 95; Springer, 2005; pp 177−199, DOI: 10.1007/b102214.
(33) Sustr, D.; Duschl, C.; Volodkin, D. A FRAP-based evaluation of protein diffusion in polyelectrolyte multilayers. *Eur. Polym. J.* **2015**, *68*, 665−670.
(34) Nazaran, P.; Bosio, V.; Jaeger, W.; Anghel, D.; v. Klitzing, R. Lateral mobility of polyelectrolyte chains in multilayers. *J. Phys. Chem. B* **2007**, *111*, 8572−8581.
(35) Masaro, L.; Zhu, X. Physical models of diffusion for polymer solutions, gels and solids. *Prog. Polym. Sci.* **1999**, *24*, 731−775.
(36) Tseng, K.; Turro, N.; Durning, C. Tracer diffusion in thin polystyrene films. *Polymer* **2000**, *41*, 4751−4755.
(37) Soumpasis, D. Theoretical analysis of fluorescence photobleaching recovery experiments. *Biophysical journal* **1983**, *41*, 95−97.
(38) Kitamura, A.; Kinjo, M. Determination of diffusion coefficients in live cells using fluorescence recovery after photobleaching with wide-field fluorescence microscopy. *Biophysics and Physicobiology* **2018**, *15*, 1−7.
(39) Karlsson, O.; Stubbs, J.; Karlsson, L.; Sundberg, D. Estimating diffusion coefficients for small molecules in polymers and polymer solutions. *Polymer* **2001**, *42*, 4915−4923.
(40) Suhling, K.; Hirvonen, L. M.; Levitt, J. A.; Chung, P.-H.; Tregidgo, C.; Le Marois, A.; Rusakov, D. A.; Zheng, K.; Ameer-Beg, S.; Poland, S.; et al. Fluorescence lifetime imaging (FLIM): Basic concepts and some recent developments. *Medical photonics* **2015**, *27*, 3−40.
(41) Woodward, W. H. Broadband Dielectric Spectroscopy: A Modern Analytical Technique. *ACS Symp. Ser.* **2021**, *1375*, 3−59.
(42) Lunkenheimer, P.; Loidl, A. Dielectric spectroscopy of glass-forming materials: α-relaxation and excess wing. *Chem. Phys.* **2002**, *284*, 205−219. Strange Kinetics.
(43) Chen, Q.; Tudryn, G. J.; Colby, R. H. Ionomer dynamics and the sticky Rouse model. *J. Rheol.* **2013**, *57*, 1441−1462.
(44) Chen, Q.; Bao, N.; Wang, J.-H. H.; Tunic, T.; Liang, S.; Colby, R. H. Linear viscoelasticity and dielectric spectroscopy of ionomer/plasticizer mixtures: a transition from ionomer to polyelectrolyte. *Macromolecules* **2015**, *48*, 8240−8252.
(45) Tudryn, G. J.; O'Reilly, M. V.; Dou, S.; King, D. R.; Winey, K. I.; Runt, J.; Colby, R. H. Molecular mobility and cation conduction in polyether−ester−sulfonate copolymer ionomers. *Macromolecules* **2012**, *45*, 3962−3973.
(46) Klein, R. J.; Runt, J. Plasticized single-ion polymer conductors: conductivity, local and segmental dynamics, and interaction parameters. *J. Phys. Chem. B* **2007**, *111*, 13188−13193.
(47) Deshmukh, K.; Sankaran, S.; Ahamed, B.; Sadasivuni, K. K.; Pasha, K. S.; Ponnamma, D.; Sreekanth, P. R.; Chidambaram, K. *Spectroscopic Methods for Nanomaterials Characterization*; Elsevier, 2017; pp 237−299.
(48) Kumbhakar, K.; Pham, T. D.; Lee, K.-K.; Kwak, K.; Cho, M. Dielectric relaxation spectroscopy for the characterization of ion transport in solid polymer electrolytes in Li-ion cells. *Electrochim. Acta* **2023**, *462*, 142759.
(49) Pinto, G.; Helal, E.; Ribeiro, H.; David, E.; Fechine, G.; Demarquette, N. Use of Kramers-Kronig Transform and Vogel-Fulcher-Tammann equation to probe the molecular dynamics of polyamide 10.10 nanocomposites. *2023 IEEE Conference on Electrical Insulation and Dielectric Phenomena (CEIDP)*; IEEE, 2023; pp 1−4, DOI: 10.1109/CEIDP51414.2023.10410559.
(50) Kremer, F.; Schönhals, A. *Broadband Dielectric Spectroscopy*; Springer Science & Business Media, 2002.
(51) Wang, Y.; Fan, F.; Agapov, A. L.; Saito, T.; Yang, J.; Yu, X.; Hong, K.; Mays, J.; Sokolov, A. P. Examination of the fundamental relation between ionic transport and segmental relaxation in polymer electrolytes. *Polymer* **2014**, *55*, 4067−4076.
(52) Chang, B.-Y. The Effective Capacitance of a Constant Phase Element with Resistors in Series. *J. Electrochem. Sci. Technol.* **2022**, *13*, 479−485.
(53) Havriliak, S.; Negami, S. A complex plane representation of dielectric and mechanical relaxation processes in some polymers. *Polymer* **1967**, *8*, 161−210.
(54) Volkov, A. S.; Koposov, G.; Perfil'ev, R.; Tyagunin, A. Analysis of experimental results by the Havriliak−Negami model in dielectric spectroscopy. *Opt. Spectrosc.* **2018**, *124*, 202−205.
(55) Volkov, A. S.; Koposov, G.; Perfiliev, R. On the physical meaning of disperse parameters of frequency dependence of dielectric permittivity in the Havriliak−Negami model. *Opt. Spectrosc.* **2018**, *125*, 379−382.
(56) Wang, H.; Liu, H.; Cao, Z.; Li, W.; Huang, X.; Zhu, Y.; Ling, F.; Xu, H.; Wu, Q.; Peng, Y.; et al. Room-temperature autonomous self-healing glassy polymers with hyperbranched structure. *Proc. Natl. Acad. Sci. U. S. A.* **2020**, *117*, 11299−11305.
(57) Rathi, A.; Dierkes, W.; Blume, A.; Hernandez, M.; Bergmann, C.; Trimbach, J. Structure−property relationships of 'safe' aromatic oil based passenger car tire tread rubber compounds. *KGK Kautschuk, Gummi, Kunststoffe* **2016**, *69*, 22−27.
(58) Sheha, E. Ionic conductivity and dielectric properties of plasticized PVA0. 7 (LiBr) 0.3 (H2SO4) 2.7 M solid acid membrane and its performance in a magnesium battery. *Solid State Ionics* **2009**, *180*, 1575−1579.
(59) Mal'chevskii, V.; Regel', V.; Zheleznov, V.; Fal'kovskii, M. Effect of plasticization on the activation energy of failure of nitrocellulose. *Polymer Mechanics* **1973**, *9*, 313−316.
(60) Du, Z.; Chen, X. C.; Sahore, R.; Wu, X.; Li, J.; Dudney, N. J. Effects of plasticizer content and ceramic addition on electrochemical properties of cross-linked polymer electrolyte. *J. Electrochem. Soc.* **2021**, *168*, No. 050549.
(61) Ginzburg, V. V. A simple mean-field model of glassy dynamics and glass transition. *Soft Matter* **2020**, *16*, 810−825.

https://doi.org/10.1021/acs.macromol.5c01318
Macromolecules XXXX, XXX, XXX−XXX

(62) Jiang, J.; Lu, Z.; Shen, J.; Wada, T.; Kato, H.; Chen, M. Decoupling between calorimetric and dynamical glass transitions in high-entropy metallic glasses. *Nat. Commun.* **2021**, *12*, 3843.
(63) Qiao, J.; Chen, Y.; Casalini, R.; Pelletier, J.; Yao, Y. Main α relaxation and slow β relaxation processes in a La30Ce30Al15Co25 metallic glass. *Journal of Materials Science & Technology* **2019**, *35*, 982−986.

https://doi.org/10.1021/acs.macromol.5c01318
Macromolecules XXXX, XXX, XXX−XXX